Minireview

Mechanics of coupling proton movements to *c*-ring rotation in ATP synthase

Robert H. Fillingame*, Christine M. Angevine, Oleg Y. Dmitriev

Department of Biomolecular Chemistry, 1300 University Avenue, University of Wisconsin Medical School, Madison, WI 53706, USA

Received 25 August 2003; accepted 1 September 2003

First published online 6 October 2003

Edited by Gunnar von Heijne, Jan Rydström and Peter Brzezinski

Abstract **F_1F_0 ATP synthases generate ATP by a rotary catalytic mechanism in which H^+ transport is coupled to rotation of an oligomeric ring of *c* subunits extending through the membrane. Protons bind to and then are released from the aspartyl-61 residue of subunit *c* at the center of the membrane. Subunit *a* of the F_0 sector is thought to provide proton access channels to and from aspartyl-61. Here, we summarize new information on the structural organization of *Escherichia coli* subunit *a* and the mapping of aqueous-accessible residues in the second, fourth and fifth transmembrane helices (TMHs). Aqueous-accessible regions of these helices extend to both the cytoplasmic and periplasmic surface. We propose that *a*TMH4 rotates to alternately expose the periplasmic or cytoplasmic half-channels to aspartyl-61 of subunit *c* during the proton transport cycle. The concerted rotation of interacting helices in subunit *a* and subunit *c* is proposed to be the mechanical force driving rotation of the *c*-rotor, using a mechanism akin to meshed gears.**

Key words: ATP synthase; Proton transport; Rotary motor; Aqueous access channel; Cysteine chemical modification; Subunit *a*; Subunit *c*

1. Introduction

H^+-transporting, F_1F_0-type ATP synthases utilize a transmembrane H^+ potential to drive ATP formation by a rotary catalytic mechanism [1]. ATP is formed in the F_1 sector of the enzyme, synthesis being driven by rotation of the γ subunit between three alternating catalytic sites (Fig. 1). Recent evidence now supports a mechanism in which H^+ transport drives rotation of an oligomeric ring of 10 *c* subunits in the F_0 sector of the enzyme, which in turn is coupled to rotation of subunit γ [3–6]. In such a model [7–9], the sequential protonation and deprotonation of Asp61 of subunit *c* is coupled with a stepwise movement of the rotor. Protons are thought to gain access to Asp61 in the center of the membrane via access channels that are at least partially located in subunit *a*. The γ subunit is forced to turn with the *c*-ring due to an apparently permanent binding between the γ and ε subunits of F_1 and a set of *c* subunits of the ring [6]. In this essay we will summarize recent studies that bear on the mechanism of *c*-ring rotation, and postulate that a meshed turning of transmembrane α-helices drives the *c*-ring rotation, akin to the rotation of meshed gears.

Subunit *c* folds in the membrane as a hairpin of two extended transmembrane helices (TMHs) with the proton carrying Asp61 centered in *c*TMH2. A nuclear magnetic resonance (NMR) structure of the purified monomeric protein depicts the predicted helical hairpin with inter-helical residue interactions consistent with those predicted for the protein in situ [10], and the model fits well with an extensive set of genetically introduced disulfide cross-links [11]. The cross-linking data were also used to model the *c*-ring [12,13]. The number of *c* subunits in the ring is controversial and may vary between species. Our most recent experiments suggest that the preferred number in *Escherichia coli* is 10, based upon cross-linking of functional genetically fused c_3 and c_4 oligomers [14]. The cross-link-based models of the *c*-oligomer show a ring of subunits with TMH1 on the inside and TMH2 on the outside. The placement of TMH2 on the outside is supported by other cross-linking studies in which TMH4 of subunit *a* can be cross-linked to *c*TMH2 at multiple points over a span of 19 amino acid residues [15]. The NMR structure and *c*-ring models are now supported by direct crystallographic observations of a mitochondrial F_1–c_{10} subcomplex at 3.9 Å resolution [16] and a two-dimensional, crystallographic analysis of the purified *Ilyobacter tartaricus* c_{11} ring, crystallized in the absence of subunits *a* and *b* [17].

In the model of the *c*-ring, the H^+-carrying carboxyl of subunit *c* is occluded between neighboring subunits [12]. The subunits are arranged, with an ellipsoid-like cross-section, where the Asp61 side chain at the '*front*' side of one subunit packs at the '*back*' face of the next subunit (Fig. 2). In the case of *E. coli*, the packing meets the required functional interactions of residues 24 and 28 of TMH1 with Asp61 of TMH2 in DCCD resistant mutants [18], and the predicted interaction of residues 62 and 61 in a Li^+ binding mutant [19] (see Fig. 2). In the case of the *I. tartaricus* *c*-ring, the packing is predicted to result in the binding of Na^+ between residues equivalent to *E. coli* residue 61 of TMH2 at the *front* face of one subunit and TMH1 residue 28 and TMH2 residue 62 at the *back* face of a second subunit [17]. In order for protons to gain access to Asp61 during the H^+-transport cycle, we have proposed that the outer, Asp61-bearing

*Corresponding author. Fax: (1)-608-262 5253.
E-mail address: rhfillin@facstaff.wisc.edu (R.H. Fillingame).

Abbreviations: NEM, *N*-ethyl-maleimide; TMH, transmembrane helix

0014-5793/03/$22.00
doi:10.1016/S0014-5793(03)01101-3

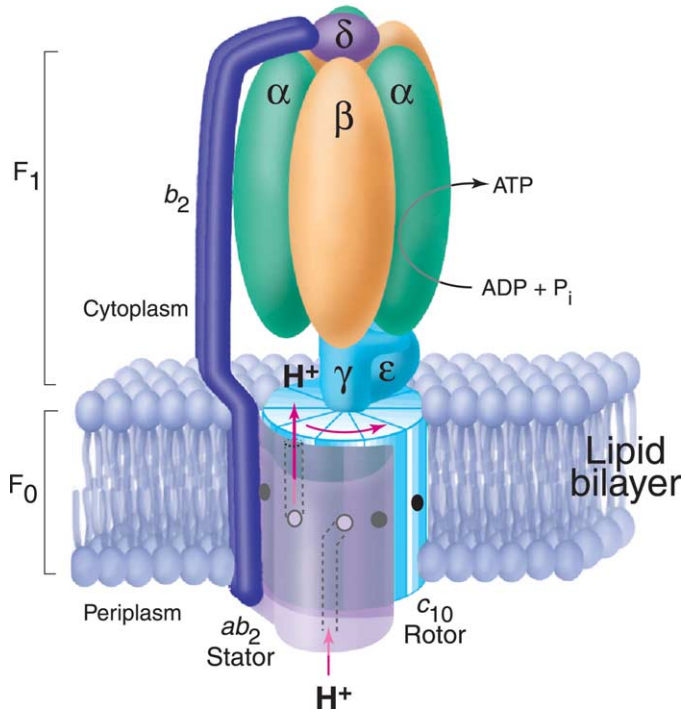

Fig. 1. Rotary model for how *E. coli* F_1F_0 ATP synthase catalyzes formation of ATP (adapted from [2]). Rotation of the c_{10} oligomeric ring is driven by the proton-motive force. Protons enter the assembly through the periplasmic inlet channel and bind to the Asp61 carboxylate (open circle). The protonated binding site (filled circle) then moves from the a_1b_2 stator component towards the lipid phase of the membrane where, after 10 steps, it reaches an outlet channel on the cytoplasmic side of the membrane to release the proton. The γ and ε subunits are proposed to remain fixed to the top of one set of *c* subunits so that rotation of the rotor also drives rotation of subunit γ within the $\alpha_3\beta_3$ subunits of F_1 to cause release of ATP from the alternating catalytic sites. The b_2 and δ subunits of the stator hold the $\alpha_3\beta_3$ subunits in a fixed position as the γ subunit turns within to drive ATP synthesis.

TMH2s of the *c*-ring must turn or swivel to allow interaction with the Arg210 residue of subunit *a*, which is hypothesized to lower the pK_a of *c*Asp61 to enable ionization and H^+ release to the exit channel [20,21]. In this minireview, we present evidence that TMHs in subunit *a* may have to rotate to gate movement of protons from the entrance and exit channels. In addition, we will incorporate NMR structures of subunit *c* in several states in proposing a mechanistic model by which H^+-transport and the concerted swiveling of helices in subunits *c* and *a* are linked to the stepwise rotational movement of the *c*-rotor.

2. Arrangement of TMHs in subunit *a*

A model for the cross-sectional arrangement of four of the five TMHs of subunit *a* is shown in Fig. 2. The model is based upon the theoretical helical wheels for the defined TMHs of subunit *a* and a series of second-site-suppressor mutations that restore function in primary mutants [21]. The second-site-suppressor pairs could indicate a physical juxtaposition of interacting residues. The mutational pairs that fit the model well are: residue 218 in TMH4 with residue 245 in TMH5, residue 219 in TMH4 with residue 145 in TMH3, and residue 245 in TMH5 with residue 119 in TMH2. Rastogi and Girvin [13] have used the same data set as distance constraints in molecular mechanics and energy minimization calculations to generate a three-dimensional model for TMH interaction. Despite some conflicting evidence [21], we now believe that the arrangement shown is a good working model, this conclusion being based upon disulfide cross-linking of Cys residues substituted in the vicinity of the second-site-suppressor mutational pairs, i.e. Cys–Cys cross-links between TMHs 2 and 4, TMHs 2 and 5, and TMHs 4 and 5 (B. Schwem and R.H. Fillingame, in preparation).

3. Aqueous access to the interior from both faces of subunit *a*

We have used *N*-ethyl-maleimide (NEM) and Ag^+ as probes of aqueous accessibility of Cys residues substituted into continuous stretches of residues in TMHs 2, 4 and 5 [22,23]. NEM and Ag^+ react preferentially with the ionized thiol group, and hence reactive residues are presumed to reside in a polar, aqueous-accessible environment. NEM was found to preferentially react with Cys206, 210 and 214 at the peripheral face of *a*TMH4 in the four-helix bundle shown in Fig. 2. NEM reaction led to inhibition of ATPase-coupled H^+-transport in membrane vesicles from the *a*S206C and *a*N214C mutants [22]. The *a*R210C mutation itself leads to loss of function, and NEM reactivity was demonstrated by labeling with [^{14}C]NEM [22]. Other residues in *a*TMH4 proved to be considerably less reactive to NEM. Residues 206, 210 and 214 extend from the cytoplasmic face to the center of the lipid bilayer in the topological model shown in Fig. 3, and most simply suggest aqueous access from the cytoplasm to the central core of subunit *a* via these and perhaps other residues. Ag^+ has also been used as a probe of aqueous

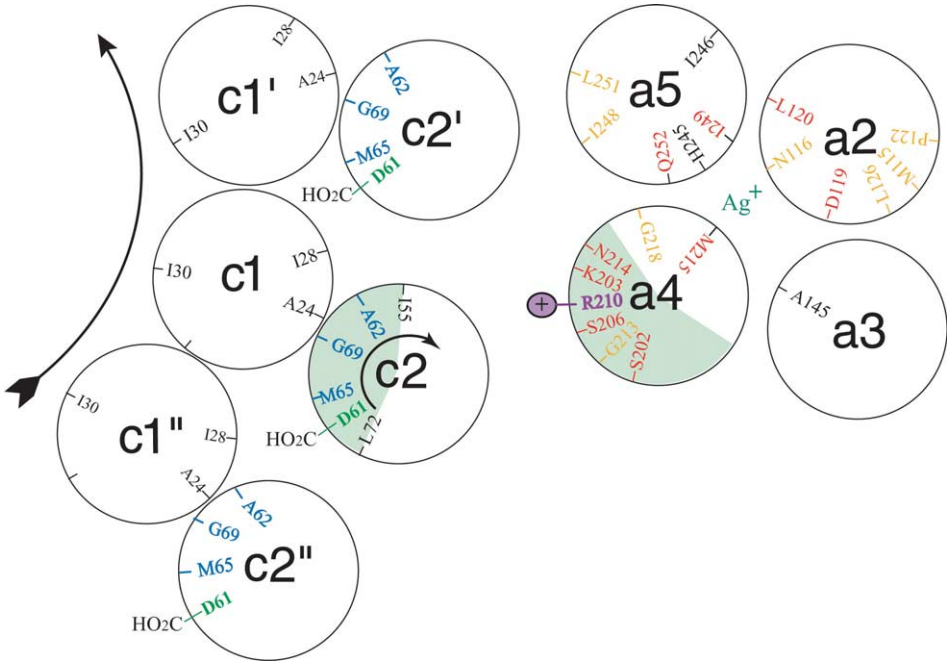

Fig. 2. Cross-sectional model of subunit *a* complexed with three *c* subunits of the *c*-ring. TMH1 of subunit *a* is not shown. The relative positions of residues interacting as second-site-suppressor pairs are indicated. NEM-sensitive residues in *a*TMH4 are described in the text. Ag^+-sensitive residues in *a*TMH2, 4 and 5 are shown in red or orange, based upon their relative reactivity (red > orange) [23]. The cross-linkable faces of *a*TMH4 and *c*TMH2 are shown in green shading. The positions of the key functional residues, *c*Asp61 and *a*Arg210 side chains are shown, and the cross-linkable residues in *c*TMH2 that are discussed in the text indicated in blue.

accessibility of Cys-substituted mutants of subunit *a*. Ag^+ is thought to react as a Lewis acid with the thiolate group to form a covalent bond. Ag^+ has an ionic radius approximating that of H_3O^+, or Na^+, which may make it an ideal probe of such access channels. ATP-driven proton transport by the NEM-sensitive mutants, *a*S206C and *a*N214C, also proved to be inhibited by Ag^+ [22]. More surprisingly, a number of mutants that were NEM-insensitive showed striking inhibition when treated with Ag^+ [22,23]. In TMH4, for example, the two mutants showing the greatest sensitivity to Ag^+, *a*M215C and *a*G218C, were totally resistant to inhibition by NEM [22]. These residues fall towards the center of the four helix bundle shown in Fig. 2, and lie opposite to the helical face for residues 206, 210 and 214. For TMH5, the most Ag^+-sensitive residues cluster at the center of the membrane, with lesser reactive residues extending to the periplasmic surface (Fig. 3; [23]). For TMH2, the Ag^+-sensitive residues extend from the center of the membrane to the periplasmic surface (Fig. 3; [23]). In the four-helix bundle model for subunit *a* (Fig. 2), the most Ag^+-sensitive residues in TMH2 and TMH4 tend to

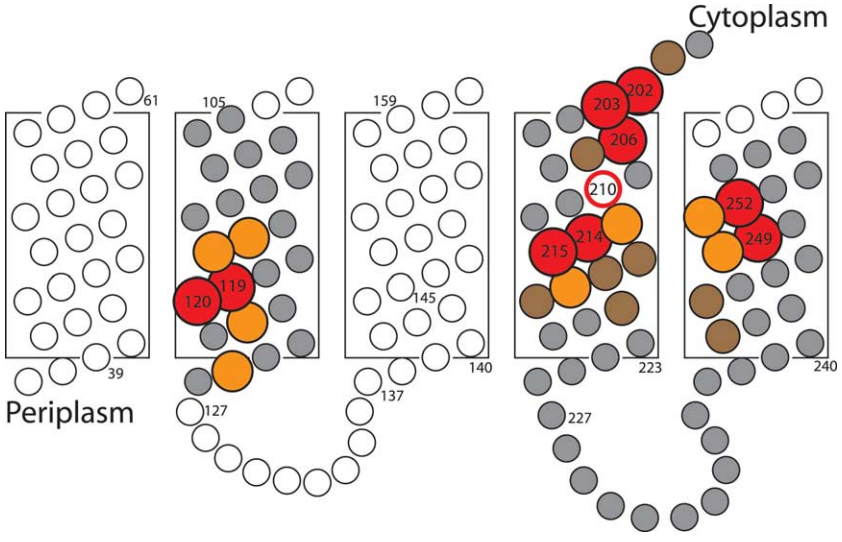

Fig. 3. Topological model for the folding of subunit *a* in the membrane (based upon [24]), and the positions of Ag^+-reactive residues [23] (reactivity scaled as red > orange > brown ≫ gray). White residues have not been tested. Many of the numbered residues are referred to in the text.

cluster at the center of the bundle, as was the case for the NEM-insensitive and Ag^+-sensitive residues in TMH5. In summary, the NEM and Ag^+-sensitive face of *a*TMH4 could provide an aqueous-access pathway from the center of the membrane to the cytoplasm, and a possible pathway of proton release from Asp61 of subunit *c* at the periphery of the *c*-rotor. In contrast, the Ag^+-sensitive and NEM-insensitive residues in TMHs 2, 4 and 5 provide a possible aqueous pathway for proton access from the periplasm to the center of the membrane, but the pathway would appear to be centered at the middle of the four-helix bundle. If protons in the periplasmic pathway are to reach *c*Asp61, the pathway would have to be gated by structural changes in the postulated four-helix bundle, perhaps by the swiveling of helices.

4. Evidence for interaction of *c*TMH2 with *a*TMH4

High-yield disulfide cross-links can be formed between Cys residues introduced into *c*TMH2 and *a*TMH4, where the cross-linkable Cys–Cys pairs span a region 19 amino acids in both helices [15]. The cross-linkable residues extend from residues 55 to 73 in subunit *c* and residues 207 to 225 in subunit *a*. The cross-linkable residues in *a*TMH4 fall on the peripheral face of TMH4 in the four-helix bundle model of subunit *a* (Fig. 2), i.e. the NEM-sensitive face containing the essential *a*R210 residue. The cross-linkable residues in subunit *c* map to the interior face of *c*TMH2 in the oligomeric model of the *c*-ring (Fig. 2). For example, residues 62 and 65 pack at the interface with *c*TMH1, and both form cross-links with *a* N214C in high yield. Residue *c*G69C also packs at the interface with *c*TMH1 but forms a high-yield cross-link with *a* I221C. In this case, the *c*G69C mutation results in a loss of function, and one could argue that the structure of the mutant protein might be perturbed; hence the proximal positioning of residues might not apply to the native protein. Since the original study [15], we have screened for second-site suppressors with the *c*G69C mutant and remarkably found the second-site-suppressing mutation to be *a*L221H, i.e. in the same residue as that of the cross-linkable pair. The new *c*G69C/*a*I221H suppressor pair suggests that these residues may interact in a functional way.

5. Evidence for rotation of TMH2 of subunit *c*

The following observations suggest that the rotational positions of *c*TMH2 in the *c*-ring model, relative to *c*TMH1, may have to change in the course of function. The position of helices shown in the *c*-ring model is based upon distance contraints derived from inter-subunit *c*–*c* cross-linking [11,12], and the original NMR model of the monomeric protein in its protonated form [10]. Other observations leading to a suggested rotation of *c*TMH2 are:

1. The essential residue *a*Arg210 is postulated to interact with *c*Asp61 during the protonation/deprotonation cycle to transiently lower the pK_a of the proton-transporting carboxylate side chain [20]. In the oligomeric model of the *c*-ring, Asp61 packs at the interface between subunits and would appear to be shielded from a direct interaction with *a*Arg210. Rotation of *c*TMH2 could expose *c*Asp61 to the periphery of the ring and promote interaction with *a*Arg210.
2. As was described in Section 4, the interior face of *c*TMH2 in the oligomeric model of the *c*-ring is the segment that forms cross-links with *a*TMH4. A 180° rotation of *c*TMH2 would facilitate formation of the complete set of cross-links.
3. The original NMR structure of subunit *c* was solved at pH 5 where Asp61 is protonated [10]. Rastogi and Girvin [13] solved a second NMR structure at pH 8 under conditions where *c*Asp61 was known to ionize [25]. The structure at pH 8 revealed a 140° clockwise rotation of *c*TMH2 relative to *c*TMH1 when compared to the pH 5 structure. In the pH 5 structure, the Asp61 side chain packs on the *front* face of the molecule, where it is thought to interact with *back* face residues of adjacent subunits of the *c*-ring to form a proton or cation binding site [10,12,17]. In the pH 8 structure, TMH2 is rotated such that the Asp61 side chain projects from the *back* face of the structure. The pH 8 structure with *c*TMH2 rotated is consistent with the *a*–*c* cross-linking data discussed above [15], and we think it is reasonable to assume that this may be the form of the protein that cross-links in situ.
4. The NMR structure of a functional aspartate-interchange mutant in which the essential Asp is moved from position 61 in TMH2 to position 24 in TMH1 was recently solved [26]. The mutant is functional [27,28], and second-site suppressors mapping to *a*TMH4 further enhance function [29]. The structure of the Asp-interchange protein is of considerable interest because retention of robust function in the various suppressors [29] implies a functional interaction between *c*TMH1 and *a*TMH4. The structure of *c*Asp24Asn61 subunit *c* was solved at pH 5 under conditions where Asp24 was fully protonated [26]. Remarkably, the structure strongly resembles that of wild-type subunit *c* at pH 8. Relative to the wild-type protein at pH 5, TMH2 has swiveled clockwise such that Asn61 packs at the *back* of the structure with TMH1 rotated enough in the opposite direction to allow the Asp24 side chain to pack at the *front* of the molecule. The new structure suggests that the swiveling of *c*TMH2, as in the pH 8 structure, is not necessarily dictated by the protonation state of the essential carboxyl group. Further, it supports the idea that the swiveling of *c*TMH2 between the two conformational states may be an important step in the mechanism.

6. Mechanical model for rotation of the *c*-ring driven by a concerted swiveling of meshed TMHs at the *a*–*c* interface

Elsewhere we have described a detailed mechanical model of how helical interactions at the *a*–*c* interface may drive *c*-ring rotation [21]. The model incorporates the rotation of *c*TMH2 between the two general structural states seen in the NMR models, and rotation of helices in subunit *a* to gate alternate aqueous-access channels from the periplasmic and cytoplasmic sides of the membrane. Rastogi and Girvin [13] have proposed a model utilizing much of the same information. We will discuss the differences in models later in this section. The major difference, and inspiring motivation leading to our model is that the same set of helix–helix interactions can be used to explain the function of the *c*Asp24Asn61 mutant, whereas the Rastogi and Girvin model does not provide an explanation for this mutant's function.

We will use the scheme in Fig. 2 to describe the model beginning with a *c*-ring in which all of the *c* subunits are

protonated. In the first step, *c*TMH2 with Asp61 protonated revolves by 140° in the *clockwise* direction with Asp61 protonated. The forces driving the helical rotation are discussed below. The helical movement enables interaction of *a*Arg210 with *c*Asp61, which lowers the pK_a of the essential carboxyl group, and following ionization of Asp61, the proton exits to the cytoplasmic side of the membrane via the *a*Ser206, NEM-sensitive exit channel at the peripheral face of *a*TMH4. At this point, the *a*Arg210 side chain must move from the vicinity of the Asp61 carboxylate such that the pK_a can rise to permit reprotonation from the periplasmic surface. The movement of the *a*Arg210 side chain is envisioned as being coupled to the simultaneous rotation of segments of *a*TMH4 (*counterclockwise*), and perhaps *a*TMH5 (*clockwise*), with a resultant exposure of *c*Asp61 to protons entering from the Ag^+-sensitive cavity at the interior of the four-helix bundle of subunit *a*. At this point, the H^+ electrochemical potential drives reprotonation of the Asp61 carboxylate via the periplasmic, Ag^+-sensitive pathway. In the final step, the concerted rotation of helices back to their original position drives the translocation of the *c*-ring one step (1/10 of 360°) in the *counterclockwise* direction. In this step *c*TMH2 and *a*TMH4 roll against each other, in a manner akin to the meshing of rotating gears, and *a*TMH4 inserts between the *c*2 and *c*2″ helices. Simultaneously, TMH2 of subunit *c*″ rotates to the position seen in the pH 8 structure. For subunit *c*″, this step is equivalent to the first step described above for the centrally located *c* subunit. With the final step, the oligomeric *c*-ring will have rotated by 36° (i.e. one unit of the rotor) relative to the stationary subunit *a* stator. The driving force for the helical rotation of *c*TMH2 is ascribed to the concerted rearrangement of all four TMHs, with the entire series of movements being coupled to proton transport driven by the proton-motive force.

There are several key differences between the model described above and that in [30], and the model of Rastogi and Girvin [13]. First, *c*TMH2 is predicted to rotate with Asp61 protonated, based upon precedent of the *c*D24N61 NMR structure, and this rotation brings Asp61 into proximity of *a*Arg210, where its pK_a is lowered to facilitate deprotonation. In the Rastogi and Girvin model, the ionization of Asp61 is suggested to cause the structural changes leading to *c*TMH2 rotation. Second, Rastogi and Girvin [13], and Fillingame et al. [30] elsewhere, have suggested that *c*TMH2 may turn in a *counterclockwise* direction by 220° to expose the Asp61 side chain to the periphery of the ring. Since an exposure of the essential aspartyl side chain to the very periphery of the ring is highly unlikely in the *c*Asp24Asn61 interchange mutant, a lesser rotation of 140° in the *clockwise* direction is suggested here.

How can the general model described above explain the structure and function of the *c*Asp24Asn61 mutant? We begin with an arrangement of helices as in the pH 5 wild-type structure except that the *c*1 helices are slightly swiveled such that Asp24 protrudes to the *front* face rather than to the *rear* face of the subunit as for Ala24 in the wild-type subunit. In the first step, TMH2 would rotate as in the wild-type model, but the movement occurs with a concerted swiveling of helices, and the movement of both the Asp24 and Asn61 side chains to the back of the molecule. This would place the Asp24 side chain in the same pocket and in the same relative position as the Asp61 side chain of the wild type in the same state. The other steps and helical movements would be identical to the description for the wild-type protein given above, and are described in greater detail in [21]. In this model, the protonated *c*Asp24Asn61 structure seen in the NMR model is observed in one of the intermediate steps. The major difference between the models for the wild type and *c*Asp24Asn61 subunits is that the turning of helix *c*2″ is accompanied by a concerted, but lesser swiveling of helix *c*1″ in the case of the mutant subunit. Conceivably, such a swiveling of both helices might also occur in the case of wild type. If a concerted turning of helices does occur in wild type, it must occur with a second swivel point located near the *c*Ile30 side chain at the inner surface of the ring. Our reasoning here is that high-yield cross-linked dimers can be formed with the *c*I30C mutant, and cross-link formation results in minimal perturbation of function [14]. The *c*Asp24Asn61 mutant may prove to be more sensitive to such cross-linking. We view the varying models as being testable, working hypotheses and expect they will change with new experimental information and structures.

Acknowledgements: We thank Kelly Gostomski-Herold and Brian Schwem for assistance in many of the experiments. Supported by US Public Health Service Grant GM23105.

References

[1] Noji, H., Yasuda, R., Yoshida, M. and Kinosita Jr., K. (1997) Nature 386, 299–302.
[2] Fillingame, R.H. (1999) Science 286, 1687–1688.
[3] Sambongi, Y., Iko, Y., Tanabe, M., Omote, H., Iwamoto-Kihara, A., Ueda, I., Yanagida, T., Wada, Y. and Futai, M. (1999) Science 286, 1722–1724.
[4] Pänke, O., Gumbiowski, K., Junge, W. and Engelbrecht, S. (2000) FEBS Lett. 472, 34–38.
[5] Tanabe, M., Nishio, K., Iko, Y., Sambongi, Y., Iwamoto-Kihara, A., Wada, Y. and Futai, M. (2001) J. Biol. Chem. 276, 15269–15274.
[6] Tsunoda, S.P., Aggeler, R., Yoshida, M. and Capaldi, R.A. (2001) Proc. Natl. Acad. Sci. USA 98, 898–902.
[7] Vik, S.B. and Antonio, B.J. (1994) J. Biol. Chem. 269, 30364–30369.
[8] Engelbrecht, S. and Junge, W. (1997) FEBS Lett. 414, 485–491.
[9] Elston, T., Wang, H. and Oster, G. (1998) Nature 391, 510–513.
[10] Girvin, M.E., Rastogi, V.K., Abildgaard, F., Markley, J.L. and Fillingame, R.H. (1998) Biochemistry 37, 8817–8824.
[11] Jones, P.C., Jiang, W. and Fillingame, R.H. (1998) J. Biol. Chem. 273, 17178–17185.
[12] Dmitriev, O.Y., Jones, P.C. and Fillingame, R.H. (1999) Proc. Natl. Acac. Sci. USA 96, 7785–7790.
[13] Rastogi, V.K. and Girvin, M.E. (1999) Nature 402, 263–268.
[14] Jiang, W., Hermolin, J. and Fillingame, R.H. (2001) Proc. Natl. Acad. Sci. USA 98, 4966–4971.
[15] Jiang, W. and Fillingame, R.H. (1998) Proc. Natl. Acad. Sci. USA 95, 6607–6612.
[16] Stock, D., Leslie, A.G.W. and Walker, J.E. (1999) Science 286, 1700–2705.
[17] Vonck, J., Krug von Nidda, T., Meier, T., Matthey, U., Mills, D.J., Kuhlbrandt, W. and Dimroth, P. (2002) J. Mol. Biol. 321, 307–316.
[18] Fillingame, R.H., Oldenburg, M. and Fraga, D. (1991) J. Biol. Chem. 266, 20934–20939.
[19] Zhang, Y. and Fillingame, R.H. (1995) J. Biol. Chem. 270, 87–93.
[20] Fillingame, R.H. (1990) in: The Bacteria (Krulwich, T.A., Ed.), Vol. 12, pp. 345–391. Academic Press, New York.
[21] Fillingame, R.H., Angevine, C.M. and Dmitriev, O.Y. (2002) Biochim. Biophys. Acta 1555, 29–36.
[22] Angevine, C.M. and Fillingame, R.H. (2003) J. Biol. Chem. 278, 6066–6074.

[23] Angevine, C.M., Herold, K.A.G. and Fillingame, R.H. (2003) Proc. Natl. Acad. Sci. USA, in press.
[24] Valiyaveetil, F.I. and Fillingame, R.H. (1998) J. Biol. Chem. 273, 16241–16247.
[25] Assadi-Porter, F.M. and Fillingame, R.H. (1995) Biochemistry 34, 16186–16193.
[26] Dmitriev, O.Y., Abildgaard, F., Markley, J.L. and Fillingame, R.H. (2002) Biochemistry 41, 5537–5547.
[27] Miller, M.J., Oldenburg, M. and Fillingame, R.H. (1990) Proc. Natl. Acad. Sci. USA 87, 4900–4904.
[28] Zhang, Y. and Fillingame, R.H. (1994) J. Biol. Chem. 269, 5473–5479.
[29] Fraga, D., Hermolin, J. and Fillingame, R.H. (1994) J. Biol. Chem. 269, 2562–2567.
[30] Fillingame, R.H., Jiang, W. and Dmitriev, O.Y. (2000) J. Exp. Biol. 203, 9–17.